XIV. Communications Elements Research

TELECOMMUNICATIONS DIVISION

A. Spacecraft Antenna Research: High-Power 400-MHz Coaxial Cavity Radiators, *K. Woo*

1. Introduction

In SPS 37-48, Vol. III, pp. 238–240, and SPS 37-51, Vol. III, pp. 307–309, the design of a 400-MHz coaxial cavity radiator was described. The power-handling capability of the antenna at very low pressures was found to be 76 W in dry air and 62 W in 100% CO_2. In this article, the design of two new models of the antenna, capable of handling much higher power, is presented. One of the models being described can handle as high as 251 W in dry air, 213 W in 100% CO_2, and 186 W in the mixture of 50% CO_2 and 50% argon.

2. Antenna Design

The two new models are: (1) a flared-aperture model, a modification of the original antenna by flaring its aperture (Figs. 1a and 2a) and (2) a wide-cavity model, an antenna having a cavity width approximately twice that of the original antenna (Figs. 1b and 2b). The flared-aperture model is intended to demonstrate that the power-handling capability of a coaxial cavity radiator can be improved upon reducing the high field at and near the cavity aperture by flaring the aperture. The wide-cavity model is intended to demonstrate that the power-handling capability of a coaxial cavity radiator can be greatly improved upon reducing the overall field strength throughout the cavity by widening the cavity.

The cavity of each new model is excited by two orthogonally located metallic feed probes. To prevent breakdown between the cavity walls and the probes, each probe is surrounded completely by teflon insulator. The probes of each antenna are fed with equal power in time quadrature by a 3-dB hybrid of the incoming line, connected to the input terminals of the antenna. When energized, each antenna radiates circularly polarized waves.

3. Test Results

The radiation patterns of the right-hand and left-hand circularly polarized components at 400 MHz of each antenna are shown in Fig. 3. The gain of each antenna is lower than it should be because of the relatively high voltage standing-wave ratio (2.8 for the flared-aperture model, 2.5 for the wide-cavity model) looking into each input terminal of each antenna. When the matching is improved, the gain will be higher.

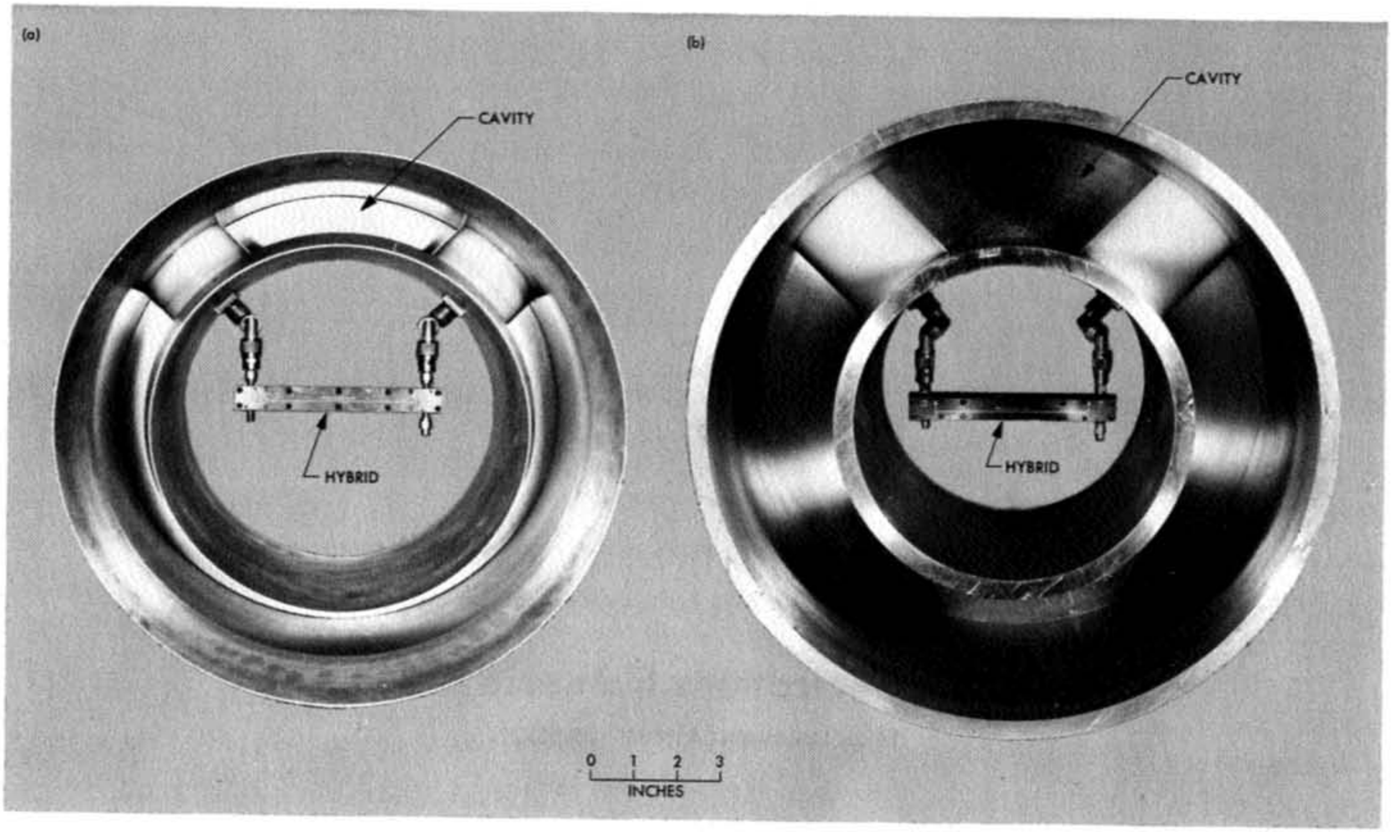

Fig. 1. Antenna model: (a) flared-aperture, (b) wide-cavity

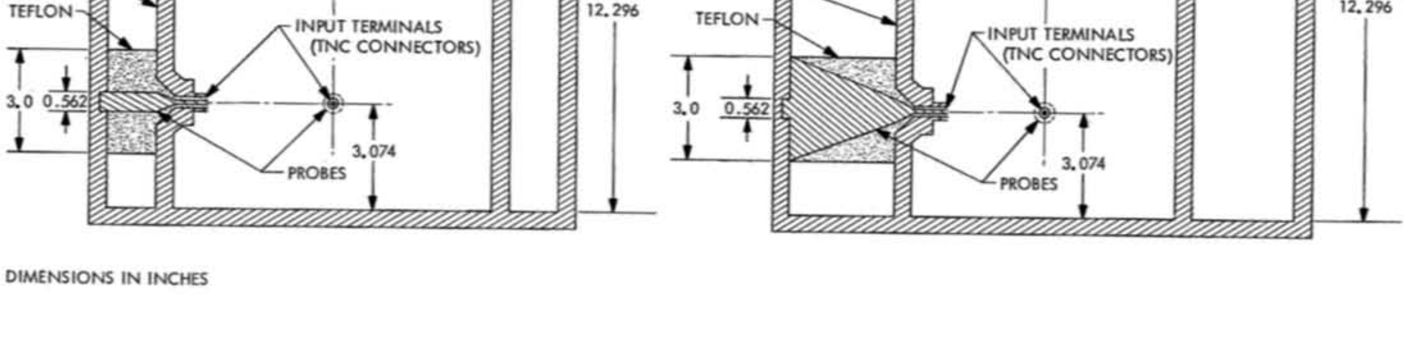

Fig. 2. Cavity and feed configuration: (a) flared-aperture model, (b) wide-cavity model

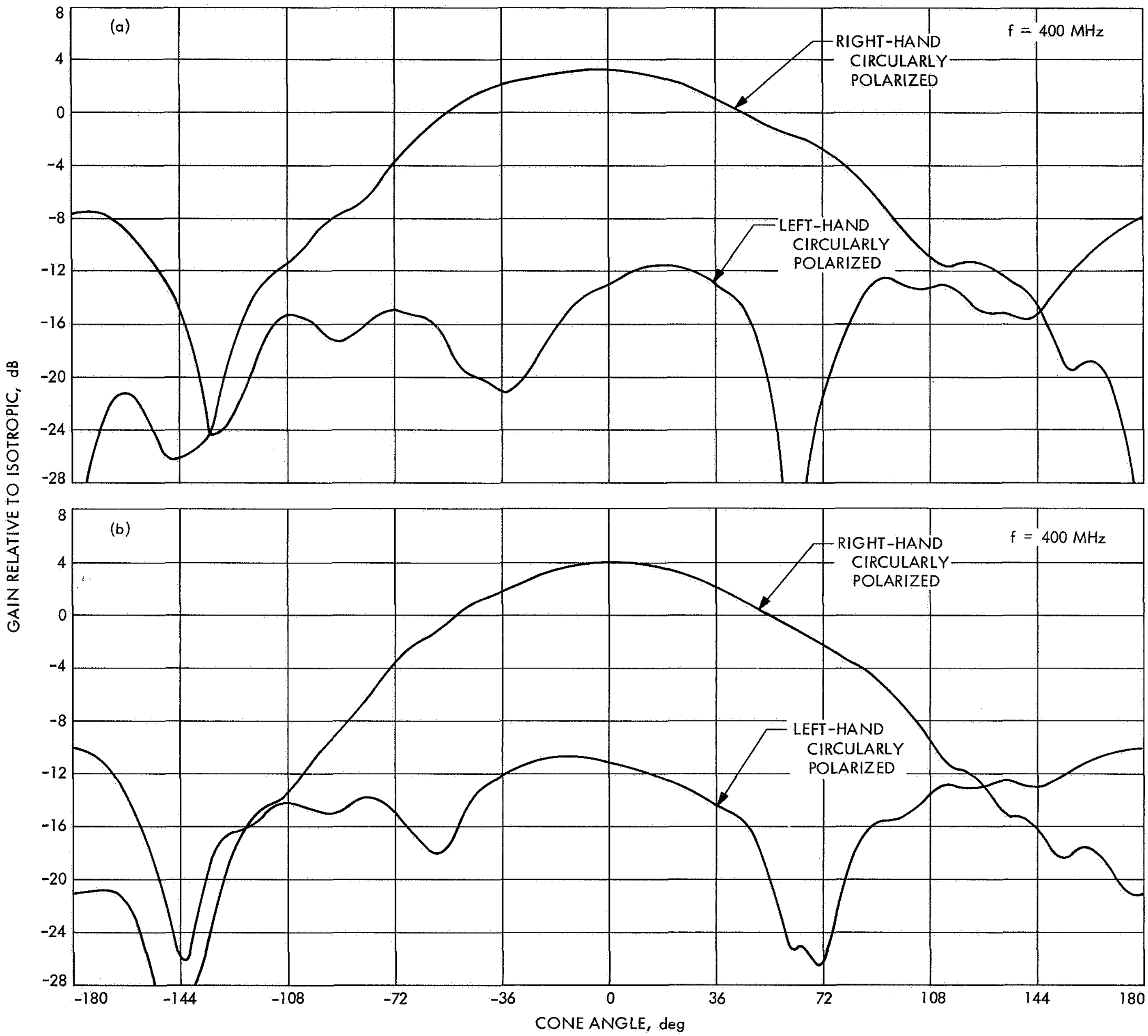

Fig. 3. Radiation patterns: (a) flared-aperture model, (b) wide-cavity model

The power-handling capabilities of the new models at very low pressures were determined in the JPL voltage breakdown facility. The antennas were each tested in the vacuum chamber with dry air, 100% CO_2, and the mixture of 50% CO_2 and 50% argon.

Figure 4 shows the ionization breakdown power level at 400 MHz of each antenna as a function of pressure near and at the point where the power-handling capability of the antenna is a minimum. These levels represent the power that each antenna cavity actually received, i.e., the power fed into the input terminals of each antenna minus the power reflected back to the hybrid as the result of mismatch.

The minimum ionization breakdown power of the flared-aperture model is 118 W (at 0.22 torr) in dry air, 97 W (at 0.28 torr) in 100% CO_2, and 84 W (at 0.33 torr) in the mixture of 50% CO_2 and 50% argon. The minimum ionization breakdown power of the wide-cavity model is

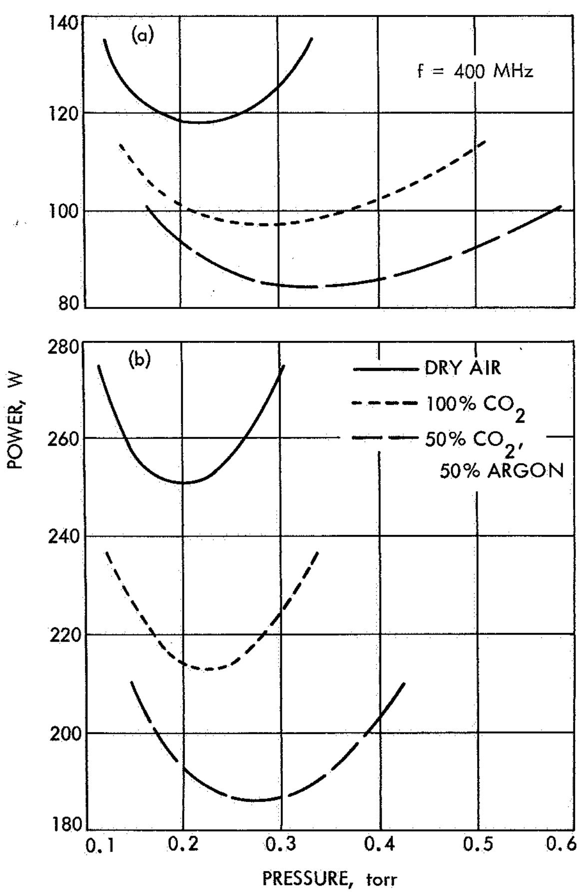

Fig. 4. Ionization breakdown characteristics: (a) flared-aperture model, (b) wide-cavity model

251 W (at 0.20 torr) in dry air, 213 W (at 0.23 torr) in 100% CO_2, and 186 W (at 0.28 torr) in the mixture of 50% CO_2 and 50% argon. In all cases, the breakdown took place around the probes as well as in the middle of the cavity.

The multipacting breakdown (tested around 8×10^{-5} torr) was not observed at 400 MHz up to a power level of 124 W for the flared-aperture model and 320 W for the wide-cavity model. These values also represent the power that each antenna cavity actually received. The multipacting tests were not carried to a higher power level in each case due to the power limitation of the feeding hybrid used.

4. Conclusion

Based on the test results, it can be said that the power-handling capability of a coaxial cavity type radiator can be improved by flaring its aperture, and can be greatly improved by widening the overall cavity width within the limits of practicality. Further work on the antennas should improve the input voltage standing-wave ratio and the ellipticity.

B. Spacecraft Antenna Research: Sterilizable High-Impact Square-Cup Radiator, Part II, *K. Woo*

1. Introduction

The sterilizable high-impact square-cup radiator reported in SPS 37-49, Vol. III, pp. 345–347, was potted with Eccofoam PT. This foam has satisfactory thermal, mechanical, and electrical properties except that it is marginal in compressive strength in comparison with that of the balsa-wood impact limiter. Under unfavorable conditions, the foam might not be able to resist the force transmitted by the balsa wood sufficiently to prevent the balsa wood from crushing into the cup during impact. In order to provide a margin of safety, a high-strength foam, Stafoam AA 630,[1] has been under investigation for possible replacement of Eccofoam PT.

2. Test Results

The square-cup radiator potted with Stafoam AA 630 is shown in Fig. 5. The foam has a density of 30 lb/ft^3 and is sterilizable. It has electrical properties similar to those of Eccofoam PT but has a considerably higher compressive strength. A compression test of the foam when potted

[1]Distributed by Olin Chemicals.

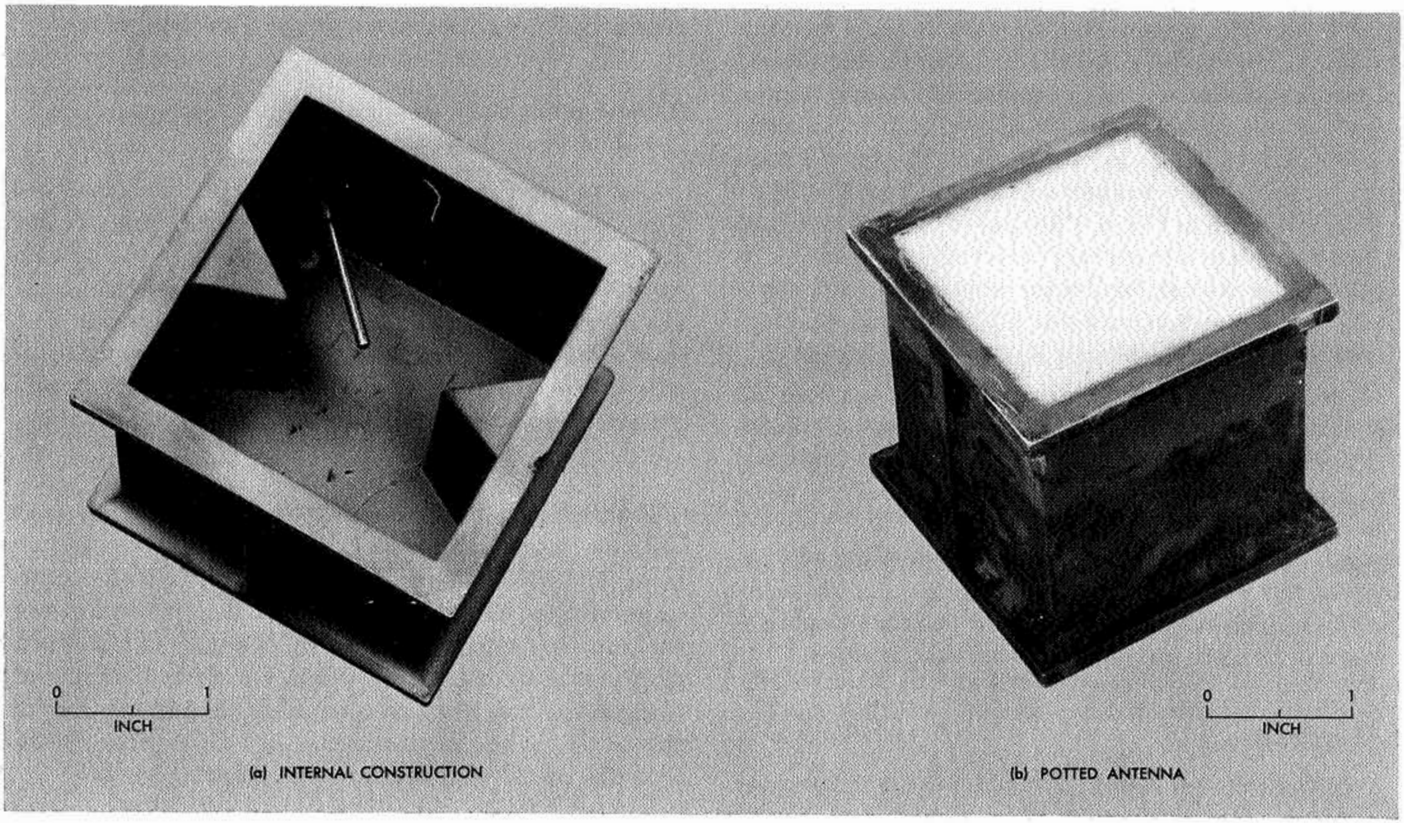

Fig. 5. Sterilizable high-impact square-cup radiator

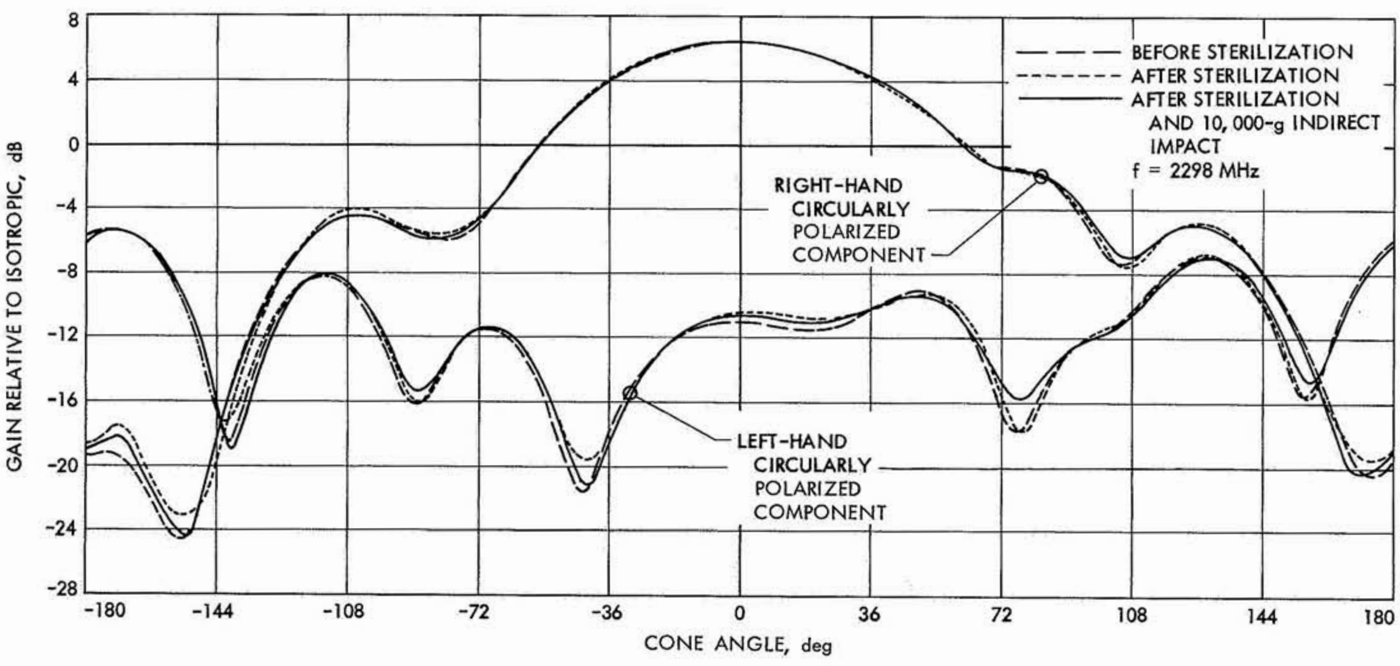

Fig. 6. Radiation patterns

in the square cup shows a compressive strength over 2,000 lb/in.[2] This is more than sufficient to resist the force transmitted by the balsa wood to prevent the balsa-wood impact limiter from crushing into the cup during impact, since the compressive strength of sterilized balsa wood is only around 1,400 lb/in.[2] on the average.[2] The electrical performance of the antenna when potted with Stafoam AA 630 is shown in Fig. 6. The dashed, dotted, and solid curves represent, respectively, the radiation patterns at 2298 MHz of the antenna before sterilization, after sterilization (70-h duration), and after 10,000-g indirect impact.

These radiation patterns show that there has been no significant change in the electrical performance of the antenna as the result of sterilization and impact. The input voltage standing-wave ratios of the antenna before sterilization, after sterilization, and after impact were, respectively, 1.60, 1.50, and 1.48. An examination of the antenna after impact revealed a few small fractures in the foam. However, the fractures were so minor that they would not influence the electrical performance of the antenna.

3. Conclusion

Based on the test results, Stafoam AA 630 is adequate for meeting the requirements of sterilizable high-impact antennas. It should be adapted for general use where high compressive strength is important. The thermal breakdown properties of the foam are presently being investigated.

C. Spacecraft Antenna Research: Large Aperture Antennas, *R. M. Dickinson*

1. Introduction

The object of this study is to determine the RF performance of erectable spacecraft antennas. For large-diameter spacecraft antennas, the resulting narrow antenna beamwidth will make it desirable to have some means of pointing the beam to earth. One method of steering the beam, that could possibly be used to remove small pointing uncertainties (such as attitude-control deadbands), consists of mechanically displacing the antenna feed at an angle to the reflector focal axis. Although the long-term reliability of a constantly moving mechanical device may be questionable, this detail implementation will not be discussed here. In any case, to cause the beam to move with respect to the reflector, the feed phase-center must be moved laterally from the focus point.

[2]Sorkin, A. B., *Effects of Sterilization on the Energy Dissipating Properties of Balsa Wood*, Technical Report 32-1295. Jet Propulsion Laboratory, Pasadena, Calif. (to be published).

2. Mechanical Beam Steering Performance in a Model Erectable Antenna

The model erectable antenna used in the experiment (Fig. 7) consists of a 6-ft-diameter radial parabolic rib antenna of 8 ribs. The ribs have a focal-length-to-diameter ratio (f/D) of 0.35. The gores or the singly curved reflecting material between the ribs are aluminized mylar. The feed consists of a column-supported circular-cupped turnstile for operation at 2297.6 MHz. Feed phase-center displacement was effected by hinging the feed column at the vertex of the reflector.

Figure 8 shows the scanning performance of the feed reflector combination. The upper abscissa is the number of beamwidths scanned. The lower abscissa is the corresponding feed tilt angle in degrees. The top curve shows the scan loss in decibels. The data of Fig. 8 is for the feed displaced along a gore center line. For the feed displaced along a rib line, the performance is, in general, similar except for slightly more scan loss (0.4 dB more at 20 deg feed tilt) but lower sidelobes (-20 dB) at 0 deg tilt.

The scan loss for the effective f/D of 0.333 is greater than existing theory (Ref. 1) predicts. This is thought to be due to the greater phase errors in the reflector surface due to modeling the paraboloid by an erectable surface. Phase errors would be expected to increase more rapidly with scan angle in the erectable antenna.

The second curve from the top in Fig. 8 shows the main lobe beamwidth as a function of scan angle. The beamwidth variation is less (Ref. 1) than normally predicted. The reason for less beamwidth changes with scan angle is at present unknown.

The center curve shows the feed voltage standing-wave ratio change with scan angle. The changes are small. The next curve down shows the sidelobe performance relative to the peak of the beam. The lower curve plots main beam angular position versus feed angular position. The almost constant scope of the curve (0.8) is the beam factor. The 0.8 beam factor agrees with theory for the effective f/D of 0.333.

Reference

1. Kelleher, K. S., and Coleman, H. P., *Off-Axis Characteristics of the Paraboloidal Reflector*, NRL Report 4088. Navy Research Laboratory, Washington, D. C., Dec. 31, 1952.

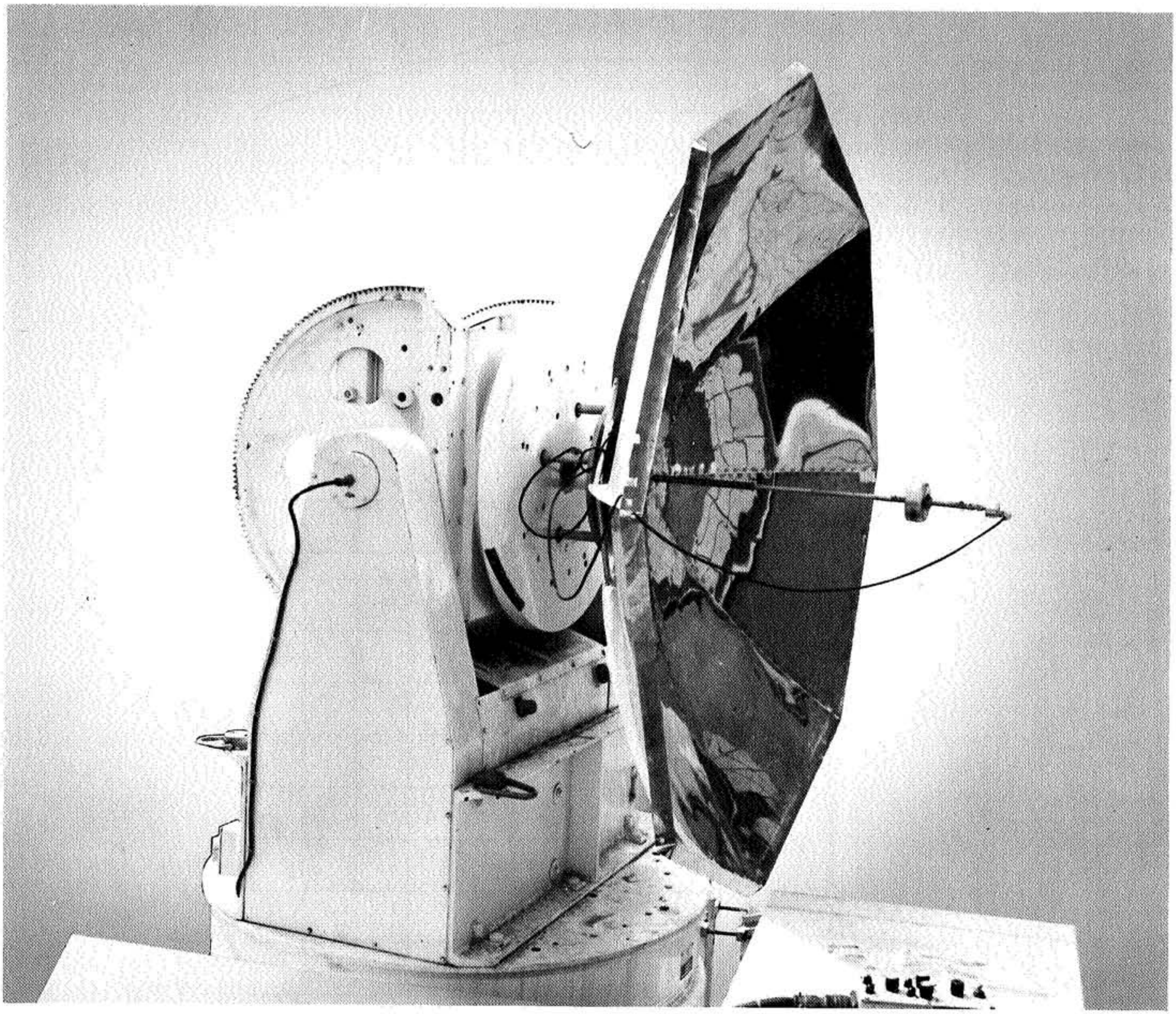

Fig. 7. 6-ft-diameter, 8-rib erectable antenna model

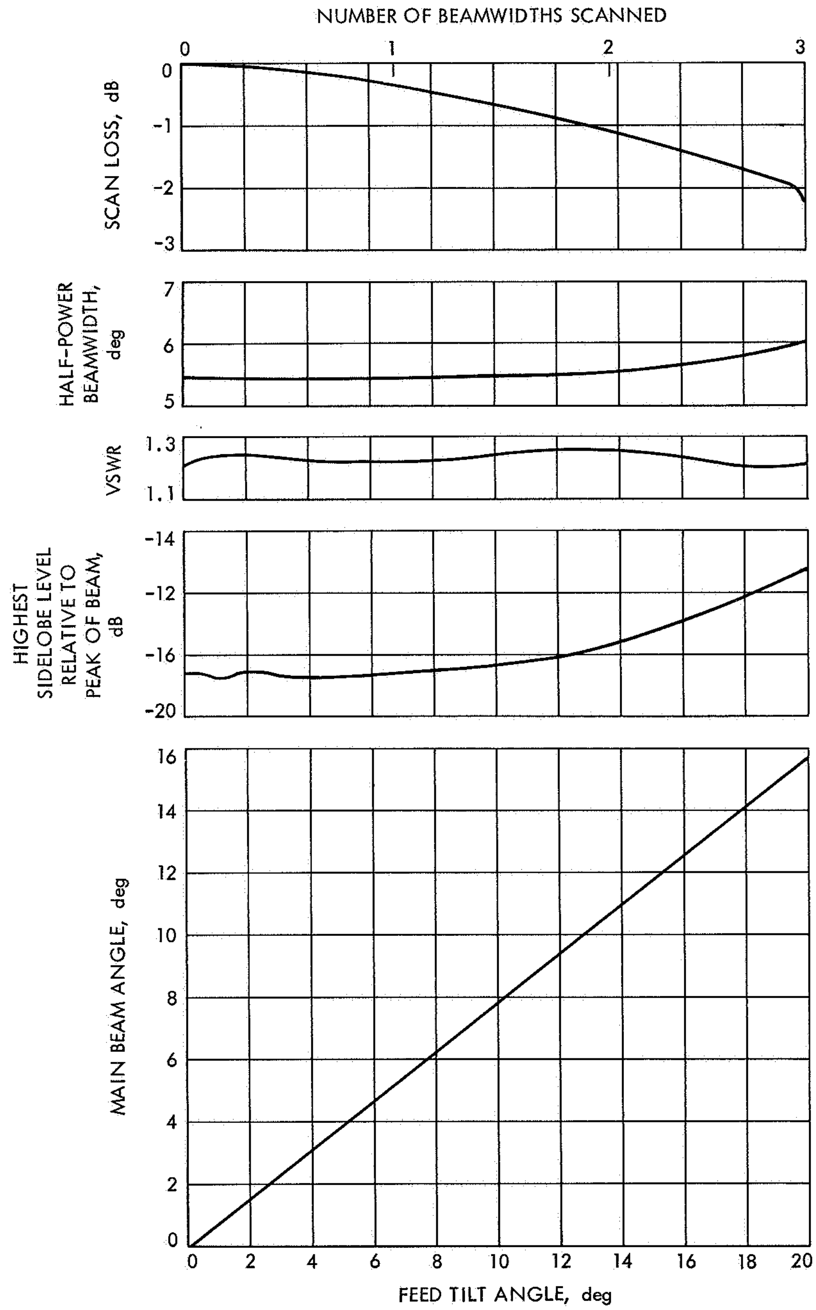

Fig. 8. Erectable reflector scanning performance